Ignition and Flame Travel on Realistic Building and Landscape Objects in Changing Environments

Mark A. Dietenberger[1]

Abstract—*Effective mitigation of external fires on structures can be achieved flexibly, economically, and aesthetically by (1) preventing large-area ignition on structures from close proximity of burning vegetations and (2) stopping flame travel from firebrands landing on combustible building objects. In using bench-scale and mid-scale fire tests to obtain fire growth properties on common building construction and landscaping plants, a model is being developed to use fast predictive methods suitable for changing environments imposed on the parcel lot consisting of structures and ornamental plants. When fully implemented and validated, the property owners and associated professionals will be able to view realistically in real-time (or faster) the various fire scenarios with the ability to select building materials and shapes as well as select ornamental plant species and placement for achieving the desired fire mitigation. Because of the analytical model's ability to respond to the changing "parcel" environments of wind, temperature, humidity, moisture, sunshine, and wildfire sources of heat and embers, as well as to variations in building construction and ornamental plants, means that analysis can be done eventually for various neighborhoods. The mathematical formulation presented at the 2006 BCC Symposium is partially shown here and some results are compared with (1) our refurbished and modified Lateral Ignition and Flame Travel Test (ASTM E1321 and E1317), (2) specialized testing of Class B burning brand (ASTM E108) in the Cone Calorimeter (ASTM E1354), (3) room-corner tests with OSB (ISO 9705), and (4) Cone Calorimeter tests of fire resistive materials such as FRT plywood and single-layer stucco-coated OSB. A preliminary Fortran dll file has been generated for use in other models, such as ecoSmart Fire.*

Introduction

With the increasing fire hazards from wildfires, particularly in Southwestern United States, the homes built in the wilderness/urban interface (WUI) will come under increasing regulatory pressures to adopt exterior fire resistive structures, in addition to managing landscape vegetation. However, it is not always clear as to the effective strategy for wildfire mitigation, even to a fire protection expert. Indeed, homeowners and builders could benefit greatly from a calculation tool for evaluating the wildfire hazards to their structures. Fire threats in the WUI basically come in two forms: (1) the long-duration exposure from firebrands spotting and (2) the short-duration exposure from heat flux and/or flame impingement of the wildfire nearing the structure.

The fire hazard threat of high heat flux or flame impingement from short-duration wildfire exposure is primarily mitigated with vegetative management in the defense zones around the combustible structure. The kind of vegetative management needed to prevent structural ignition will depend on the

In: Butler, Bret W.; Cook, Wayne, comps. 2007. The fire environment—innovations, management, and policy; conference proceedings. 26-30 March 2007; Destin, FL. Proceedings RMRS-P-46CD. Fort Collins, CO: U.S. Department of Agriculture, Forest Service, Rocky Mountain Research Station. 662 p. CD-ROM.

[1] Research General Engineer, U.S. Department of Agriculture, Forest Service, Forest Products Laboratory, Madison, WI. mdietenberger@fs.fed.us

fire resistant construction, moisture condition of landscape vegetation, and the positions/types of ornamental vegetations relative to the combustible structure. To establish the nonthreatening distances of rapidly burning ornamental vegetations away from a given structure, which may or may not be fire resistant, one should ideally use a fire hazard calculation tool, such as being partially developed in this paper. The insidious threat from long-duration firebrands' exposure, as particularly blown in from a distant huge wildfire, is really the main driving force in requiring fire resistant structures in the WUI. Obviously, the owner needs to place wire screens over chimneys, vents, and around decks and some windows to prevent ember penetration into the highly combustible interiors of buildings (Manzello and others 2006). However, it is not clear as to how much fire resistance is needed for the construction exteriors. The homeowner could well decide that the wood deck is expendable as long as the fire (possibly originating in the deck crevice with firebrands, Manzello and others 2006) does not spread into the fire resistant home. The patio door and windows should also be made resistant to the worst-case firebrand, which is likely the Class A or B simulated firebrand in the ASTM E108 test. The Class A firebrand can also be thought of as multiple firebrands collecting in a corner wall, where the upward flame spread on combustible sidings is likely. The use of an exterior FRT wood siding or similarly fire resistive material will instead prevent such flame spread, thereby limiting the damage/ignition to the region of direct exposure from the firebrands. Our main point is that reasonable and economical design of an exterior fire resistant material needs to consider the firebrand threats, even with effective vegetative management.

We believe the speed of computer computation has reached the point of bettering the real time calculation of damage, ignition, and fire growth on combustible objects. Since the CFD codes such as the Fire Dynamics Simulator are far from reaching such a point, we present here certain analytical solutions of the dynamic processes of surface heating to ignition/flame travel that leads to overall fire growth. The key numerical procedure is using stepping boundary conditions to discretize the analytical time integration and which then becomes a fully recursive computation method as a bonus. The mathematical formulation presented at the 2006 BCC Symposium (Dietenberger 2006a) is partially shown here and some results are compared with (1) our refurbished and modified Lateral Ignition and Flame Travel Test (ASTM E1321 and E1317), (2) specialized testing of Class B burning brand (ASTM E108) in the Cone Calorimeter (ASTM E1354), (3) room-corner tests with OSB (ISO 9705), and (4) Cone Calorimeter tests of fire resistive materials such as FRT plywood and single-layer stucco-coated OSB.

Ignition Predictions With Changing Conditions

The prediction of surface temperature for reaching ignition conditions that take into account the changing boundary conditions, and yet avoid the use of time-consuming finite difference methods, resulted in an innovative mathematical formulation of transient heat transfer problem. In an earlier paper (Dietenberger 2006b) we published a recursive analytical solution for transient heat and moisture transfer in a finitely thick hygroscopic material with step changes of certain boundary conditions. For many materials, moisture is not a consideration and we show here just the solution for temperature change, $T(\hat{x},t)$, profile due to boundary conditions of stepping changes in

surface heat fluxes, $\dot{q}''(\ell,t)$ and back side heat fluxes, $\dot{q}''(0,t)$, here as,

$$T(\hat{x},t) \cong \sum_{i=0}^{n} \left[\frac{\Delta\dot{q}''(\ell,t_i)}{K_{q,\ell}} S(\alpha,\hat{x},t-t_i) - \frac{\Delta\dot{q}''(0,t_i)}{K_{q,0}} S(\alpha,\ell-\hat{x},t-t_i) \right] \tag{1}$$

where $\hat{x}$ is dimensional depth, t is current time, K_q is thermal conductivity coefficient, C_q is heat capacity, ρ is dry body density, α is thermal diffusivity, and $S(\alpha,\hat{x},t)$ is the series expansion solution,

$$S(\alpha,\hat{x},t) = \frac{\alpha t}{\ell} + \ell \left\{ \frac{3\hat{x}^2 - \ell^2}{6\ell^2} - \frac{2}{\pi^2} \sum_{n=1}^{\infty} \frac{(-1)^n}{n^2} \exp\left[\frac{-\alpha t}{1} \left(\frac{n\pi}{\ell} \right)^2 \right] \cos\left(\frac{n\pi\hat{x}}{\ell} \right) \right\} \tag{2}$$

Rarely do classical heat conduction texts discuss such stepping heat fluxes, probably because the summation in equation 1 can be burdensome. However, such texts do not offer the possibility of converting equation 1 to a recursive summation, which is simple and efficient to implement as a computer routine, which we have done for this work. If irradiance, $\dot{q}''_r$, is applied to one surface, the material responds with radiative and convective cooling on the exposed side, and conductive cooling on the unexposed side as in the boundary conditions,

$$\Delta\dot{q}''(\ell,t_i) = \begin{Bmatrix} \alpha_{s,i}\dot{q}''_r(t_i) + \varepsilon_{s,i}\sigma[T_a{}^4(t_i) - T^4(\ell,t_i)] + h_{c,i}[T_a(t_i) - T(\ell,t_i)] \\ -H(t_i - t_1)\left\{ \alpha_{s,i}\dot{q}''_r(t_{i-1}) + \varepsilon_{s,i}\sigma[T_a{}^4(t_{i-1}) - T^4(\ell,t_{i-1})] + h_{c,i}[T_a(t_{i-1}) - T(\ell,t_{i-1})] \right\} \end{Bmatrix} \tag{3},$$

$$\Delta\dot{q}''(0,t_i) = C_{insulate}[T(0,t_i) - T_a(t_i)] - H(t_i - t_1)C_{insulate}[T(0,t_{i-1}) - T_a(t_{i-1})]$$

then eventually the predicted surface temperatures will reach a steady-state value in which the convective and radiative heat losses to the air and conductive heat losses to backside insulation is equal to radiant energy absorbed. The heaviside function, $H(t_i - t_1)$, is used to specify that prior to heat exposure the sample is at a uniform temperature, and therefore has zero heat fluxes at both surfaces. If the irradiance is high enough, then the surface will reach ignition temperature, T_{ig}, prior to reaching steady state temperature. To more accurately capture the time at ignition, we used time steps of one second or less, although a large time step is feasible if the boundary conditions change slowly enough as with the diurnal heating cycle.

As can be seen from equation 3 the changes in the boundary conditions with time can be used. That is, we can arbitrarily vary irradiances, convective flow, atmospheric temperature, and surface conditions with time. The method can also be extended to multilayered samples in which interfacial zones can be treated as "conductive backside cooling" heat transfers. To consider ignition due to flame impingement, we have the imposed heat flux from the 100 kW propane ignition burner (or the firebrand flames), $\dot{q}''_w$, in our room-corner burn tests to use in place of the term, $\alpha_s\dot{q}''_r + \varepsilon_s\sigma(T_a{}^4 - T(\ell,t)^4) + h_{ci}(T_a - T(\ell,t))$, in equation 3, as,

$$\dot{q}''_w = \sigma\,(\alpha_s\varepsilon_f T_f{}^4 + \varepsilon_s(1-\varepsilon_f)T_a{}^4 - \varepsilon_s T(\ell,t)^4) + h_{cf}\,(T_f - T(\ell,t)) \tag{4}$$

The parameters that are known in the case of fluxmeters in the wall are $\dot{q}''_w = 55kW/m^2$, $T(\ell,t) = 298\ K$ and absorptivity and emissivity as $\alpha_s = \varepsilon_s = 0.97$. Using averaged measured flame temperature, $T_f = 173\ K$, we derived values of flame emissivity and convective coefficient as, $\varepsilon_f = 0.391$ and $h_{cf} = 0.0165 kW/m^2\ K$ to reproduce the fluxmeter heat flux. Our test materials typically have lower surface emissivity, $\varepsilon_s = 0.88$, and using the above values for other parameters the imposed heat flux becomes 51 kW/m^2 instead. Therefore we would expect the time to ignition on the wall to correlate best with the cone heater flux of 50 kW/m^2, as was found by Karlson (1993). However, he used a multiplication factor of 1.7 times the time to ignition from the cone calorimeter to obtain the actual time to ignition for the room-corner test, which is equivalent to adding about 11 seconds (90 percent level) to ignition time due to burner lagging.

Fire Growth Simulation With Changing Conditions

In an earlier paper reporting on our ISO9705 tests (Dietenberger and Grexa 1996), we described the complex-variable Laplace transform solution of the Duhamel integral for flame spread, HRR, and pyrolysis area that involved four stages requiring solution restarts: (1) ignited corner area due to a sluggish propane burner, (2) upward spread of corner flame to the ceiling, (3) lateral spread of top-wall flame for the unlined ceiling, and (4) the preflashover rapid downward spreading of the entire three walls flame. This analytical solution was modified for application to the changing conditions of the WUI fire scenario, and the formulation reported in the 2006 BCC Symposium (Dietenberger 2006a) is briefly repeated here. First step in the analysis is the description of the extended flame flux profile as an imposed flux applied over surface distance, y_c, followed by an exponential decay with characteristic length, δ_f, as in

$$\dot{q}''_{wf}(y) = \dot{q}''_{w0}\left[H(y) + \left(\exp\left\{\frac{-(y-y_c)}{\delta_f}\right\} - 1\right) H(y-y_c)\right] \tag{5}$$

where $H(y)$ is the heaviside function. With the length of constant flux, y_c, identified with the pyrolysis front, y_p, the characteristic length was found to be proportional to extended flame length and correlated as, $\delta_f = (y_f - y_p) / c_f$, with value of c_f approximately as 1.3 for upward spread. With this spatial profile of flame heat flux, we then analyzed for the quasi-steady speed, v_p, of the pyrolysis front by using the formula, $y - y_{ig} = v_p(t_{ig} - t)$, in equation 5 to represent the sliding movement of imposed heat flux profile over a given spot until ignition temperature is reached. With this substitution, Duhamel's supposition integral is the convolution of material's thermal response to a constant imposed flux with time changing imposed flux as in

$$T_{ig} - T_m = \frac{d(T(\ell,t))}{dt} \otimes \dot{q}''_{wf}(v_p(t_{ig}-t) + y_{ig}) = (T(l,t)) \otimes \frac{d\dot{q}''_{wf}(y_{ig} - v_p(t-t_{ig}))}{dt} \tag{6}$$

where the integration is taken from zero to the time of ignition, t_{ig}, to correspond to ignition temperature, T_{ig}. We note that equation 6 becomes exactly equation 1 providing the heat flux profile of equation 5 is approximated by incremental flux changes with incremental time steps, which we will show later in evaluating the LIFT test data. Because it is possible to have a wide

variation in the characteristic flame length, depending on the direction of the flame spread, then the time step sizes will have to be highly adaptable to ensure a reasonably accurate and efficient descretization of equation 5 for its use in equation 1. If there are multiple flame spread directions on multiple combustible items, then it would be impossible to determine the optimum time steps. This is the fundamental reason why the CFD codes, such as the FDS, will fail to predict some types of flame spreading problems. To avoid this problem, the intricate analytical solution to equation 6 (instead of a discretization solution) for both thermally thick and thermally thin materials and with interpolation between the regimes is given Dietenberger (1991) as:

$$\delta_f = v_F \tau_m = v_F K_q \rho C_p \left(\frac{T_{ig} - T_m}{\dot{q}''_{w0} - \dot{q}''_{iq}} \right)^2 \left(\frac{1}{2} + \sqrt{\frac{1}{4} + \left(\frac{K_q (T_{ig} - T_m)}{\ell (\dot{q}''_{w0} - \dot{q}''_{ig})} \right)^{1.3}} \right)^{\left(\frac{-2}{1.3}\right)} \tag{7}$$

$$\text{where} \quad \dot{q}''_{ig} = \varepsilon_s \sigma (T_{ig}{}^4 - T(\ell,0)^4) + h_c (T_{ig} - T(\ell,0)) \tag{8}$$

One then realizes that all of the material's parameters for thermal response are contained in the material time constant, τ_m, during flame spreading. Closer examination of equation 7 shows that the flame travel rate, v_F, can be made quite small with large values for thermal conductivity, material density, heat capacity, material ignition temperature, and material thickness, or with small values for preheated surface temperature, flame heat flux, and flame footprint. Obviously, to completely stop flame spreading for any direction, the local flame foot heat flux has been reduced to the critical heat flux needed for ignition (via equation 8). The use of fire retardants merely improves upon this flame spread halting, even to the point of diminishing upward flame spreading under a strong radiant source. We note that supposed "constant" fire properties used in equations 7 and 8 are also changing with time, especially the flame foot and ignition fluxes.

As the next step in analytical modeling of fire growth, the flame oversize area, $A_f - A_p$, as a nonlinear function of HRR, Q_t, and flame width, w, for the corner flame (Dietenberger and Grexa 1996) is linearized at each time step as,

$$2w(y_f - y_p) = 0.0433(2w)^{1/3} Q_t{}^{2/3} \approx A_{fm} + \frac{\partial A_f}{\partial Q_t}(Q_t - Q_m) + \frac{\partial A_f}{\partial A_p}(A_p - A_{pm}) = c_f (a + b A_p + c Q_t) \tag{9}$$

The flame area for other geometries, such as the single vertical wall, a tunnel ceiling, or a circular pool fire, can be similarly linearized for their respective nonlinear functions. The fire growth problem, by rearranging equation 7, can now be stated concisely as the Voltera type integral as,

$$\frac{dA_p}{dt} = 2wv_F = \frac{a + bA_p + cQ_t}{\tau_m} + A_{ig,i} \Lambda(t - t_i) \tag{10}$$

where the total HRR is given by a sum of ignition-burner and material-flame-spreading heat release rates as,

$$Q_t = \sum_i \Delta Q_{b,i} H(t - t_i) + \sum_i A_p(t_i)\, Q''_m(t - t_i) + \int_0^{t - t_i} Q''_m(t - t_i - \xi)\, \dot{A}_p \, d\xi \tag{11}$$

$$\text{and} \quad Q''_m(t) = Q''_{m,ig} H(t) \exp(-\omega_m t) \tag{12}$$

whereas an exponentially decaying HRR profile (with decay coefficient, ω_m) is assumed for a given sample surface, with the peak HRR flux, $Q''_{m,ig}$, also changing with time as a result of the changing radiant source. The recursive Laplace solution to equation 10 given for each time step is (with $t^* = t - t_i > 0$),

$$A_p(t) = \left(\frac{a + c(Q_{mi} - A_{pi}Q''_{m,iq} + Q_{bi} + \Delta Q_{bi})}{\tau_m} + A_{pi}\omega_m\right)\left(\frac{\exp(s1t^*) - \exp(s2t^*)}{s1 - s2}\right)$$
$$+ A_{pi}\left(\frac{s1\exp(s1t^*) - s2\exp(s2t^*)}{s1 - s2}\right) + \left(\frac{a + c(Q_{bi} + \Delta Q_{bi})}{\tau_m}\right)\left(\frac{\omega_m}{s1 - s2}\right)\left(\frac{\exp(s1t^*) - 1}{s1} - \frac{\exp(s2t^*) - 1}{s2}\right) \quad (13)$$

$$Q_t(t) = Q_b(t) + Q_m(t) = Q_{bi} + \Delta Q_{bi} + \left(\frac{(a + cQ_{bi})Q''_{m,ig} - b(Q_{mi} - A_{pi}Q''_{m,ig})}{\tau_m}\right)\left(\frac{\exp(s1t^*) - \exp(s2t^*)}{s1 - s2}\right)$$
$$+ \frac{cQ''_{m,ig}}{\tau_m}\Delta Q_{bi}\left(\frac{\exp(s1t^*) - \exp(s2t^*)}{s1 - s2}\right) + Q_{mi}\left(\frac{s1\exp(s1t^*) - s2\exp(s2t^*)}{s1 - s2}\right) \quad (14)$$

where growth acceleration coefficients (in complex variable form) are,

$$s_i = \frac{b + cQ''_{m,ig} - \omega_m\tau_m}{2\tau_m} - (-1)^i\sqrt{\left(\frac{b + cQ''_{m,ig} - \omega_m\tau_m}{2\tau_m}\right)^2 + \frac{b\omega_m}{\tau_m}} \quad (15)$$

For brevity we define the recursive terms, $A_{pi} = A_{ig,\,i} + A_p(t_i)$, $Q_{bi} = Q_b(t_i)$, and $Q_{mi} = Q''_{m,ig}A_{ig,\,i} + Q_m(t_i)$. The size of the overflame area as a function of time is merely given with equation 9. Since equations 13 and 14 are framed in a recursive form, the coefficients and parameters treated as constants during a time step can be allowed to vary from time step to time step. Indeed the material time constant, τ_m, is in actuality a fairly strong function of time via the changing preheat temperature, T_m, in equation 7, which in turn is calculated with equation 1 using the time-changing external radiant flux boundary conditions. Therefore, one could conceive that the overall fire growth can switch from a damped fire spread to an accelerative fire spread, or vice versa, through the mere time variation of the material time constant. Because the roots are considered complex numbers, the above solutions are considered to be in the complex variable domain. Specialized computer algorithms were developed for complex evaluations so that the above functions could be programmed directly as a Fortran code called by the Excel spreadsheet. Because of the recursive nature of fire growth equations, it should be possible to consider various changing conditions without recalibrating the coefficients.

Class B Firebrand Tests in the Cone Calorimeter

To understand the challenges presented with a typical fire scenario in the WUI we burned the Class B firebrand of ASTM E108 in the Cone Calorimeter (ASTM E1354). A modified sample holder was used that allowed air flow into the sample as well as exposed the sample partially into the air. This necessitates us to turn the cone heater into the vertical position to keep it out of the way, and we opted not to use the cone irradiance, although we may do that in the future. Use of a Bunsen burner to ignite the brand would

have been required in the ASTM E108 test to ensure a self-burning brand, but instead for our test the brand was partially soaked in methanol bath. With ignition started at the corners of the brand, the ensuring flame took several minutes to spread around the brand. The HRR history as shown in figure 1 somewhat increases linearly to a broad peak value of 10 kW and decreases gradually afterwards. Although a simple charring wood surface has a strong initial peak HRR and then decays approximately exponentially for many seconds, the phenomenon of flame spreading around the specimen is rapid enough to result in a net increasing HRR with time. Once flame spreading is finished, the HRR should decay somewhat exponentially, but the increasing glowing HRR makes the decrease in the overall HRR to be not so rapid. The fire growth process and the effect on the HRR profile is similarly imagined for flaming vegetations, roof fires, deck fires, and so on. The challenge for analytical fire growth modeling is to reproduce the HRR profile with the use of several burning regions in the model.

The heat flux from a burning firebrand, however, varies according to size, distance, shape, viewfactor, and time-dependent HRR profile. For example, in our cone calorimeter test of Class B brand we were able to place one fluxmeter directly underneath the 150 X 150 X 60 mm wood crib with a 5 mm gap and 25 mm inward from the edge and another fluxmeter located at 45 mm outward from the wood crib. The heat flux data are shown in figure 2, which clearly shows the effects of viewfactors of the developing flame on the measured value. That is, the outside-fluxmeter seems to mimic the HRR trend and has a peak heat flux of 6.7 kW/m^2, which is not enough to ignite most materials but can still char some materials. On the other hand, the underneath-fluxmeter at first could not view the flame, and when the flame came into view, the flux levels eventually reached 50 kW/m^2. Then after the flame subsided and the wood crib was glowing throughout, the flux became as high as 80 kW/m^2. This is the high flux that rapidly ignites most materials, and also some fire resistant materials, albeit with a little more time to ignition.

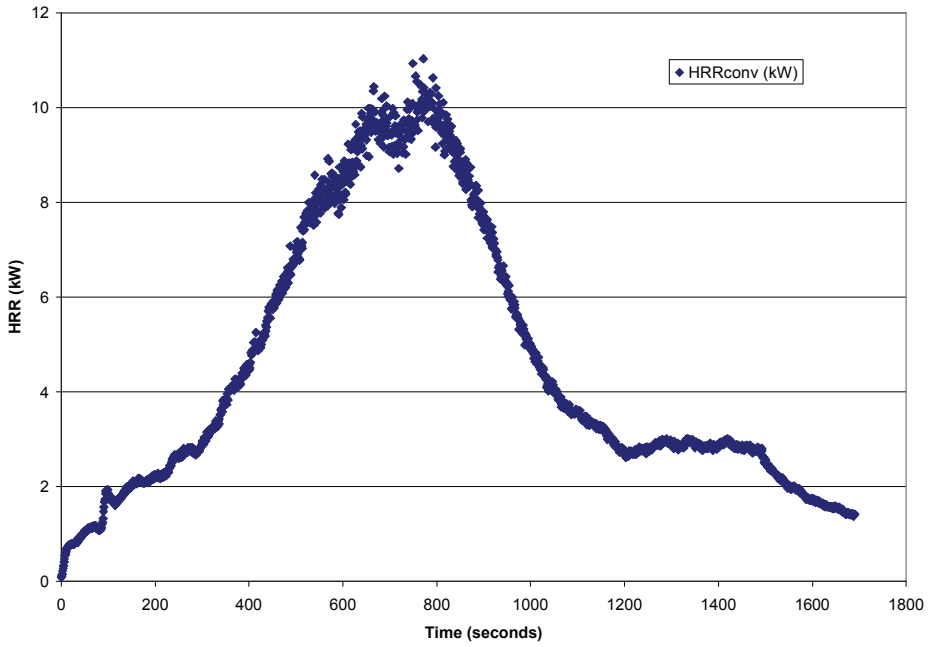

Figure 1—Heat release rate of class A brand.

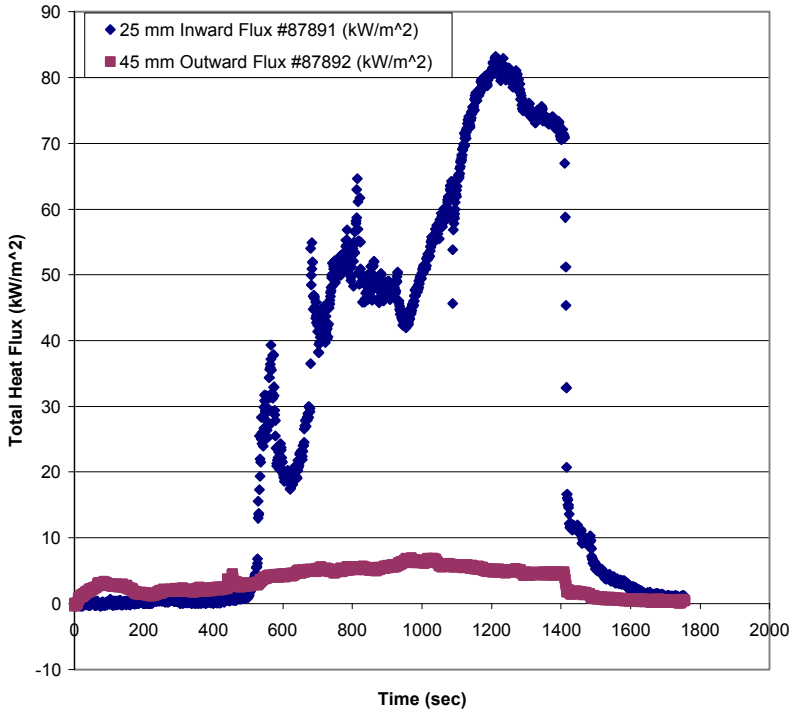

Figure 2—"A" brand heat fluxes.

Figure 3 shows the surface temperature response of dried redwood decking as calculated with equation 1 using the imposed heat flux profiles from figure 2 as the time dependent input data. The high temperatures obtained under the 80 kW/m^2 flux from the contact with wood crib glowing confirm the assertion that most combustible building materials will ignite. Yet, at a short distance away, the imposed heat flux exposure drops to the levels such that most combustible materials will not ignite.

These facts would place exterior cladding surfaces such as roofs and decks and unprotected interior flooring as highly susceptible to ignition by the "worse-case" firebrand. Therefore, designing fire resistant claddings to prevent flame spreading or avoid fire penetrating through the exposed layer after the inevitable ignition would be a desirable trait. Indeed, at least among wood materials, one could observe similar ignition behavior among different species, but that their flame spreading behavior is remarkably different.

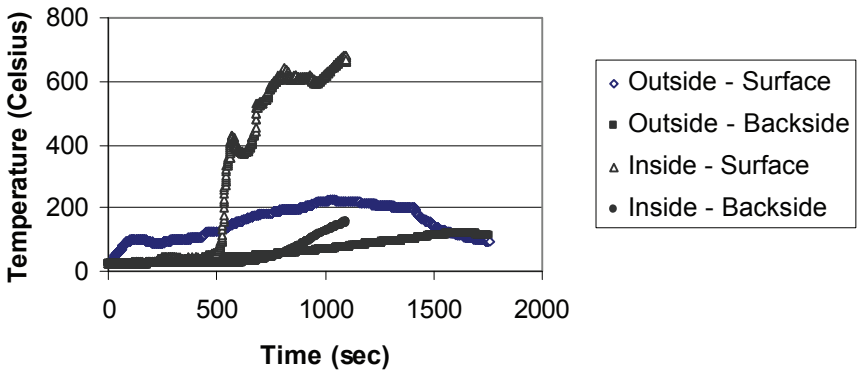

Figure 3—Analytical prediction of dried redwood response to class B brand heat exosure.

Refurbished Lift Apparatus and Analysis

Almost a couple decades ago we built the LIFT apparatus to duplicate the original at NIST BFRL, which was developed mainly by Margaret Harkleroad. The intent was to follow the ASTM E1321 standard to obtain ignition and flame spread properties for wood based materials. The standard called for the 6 inch by 30 inch vertically mounted specimen to be exposed continuously to the burner radiant heat until there was a distribution of surface temperature in equilibrium. This distribution of temperature then gave rise to a variation of lateral flame travel rate, which was to be measured manually. However, at the heat fluxes required, the wood was experiencing surface charring, which negated possibility of deriving flame travel property. Another factor creating difficulties was the unrealistic high convective flow exposures to cause ignition and flame travel, as compared to, for example, the low convective flow involving vitiated hot air in the lateral flame travel phase in the Room Corner test (ISO9705). Finally, we were dependent on the venturi tube to control the burner output with the air flow valve, which created a problem for us when the cyclic central air source caused a highly wandering burner output.

With the current emphasis on the WUI applications, installation of a mass flow controller on the air source, and utilization of faster and more accurate data acquisition, we embarked on refurbishing the LIFT apparatus. Our modified test protocol involves no surface preheating, numerous tiny surface thermocouples, and a crank-operated computer-recorded indicator for tracking flame position as function of time. The first detailed test involved the OSB that was set aside for the LIFT tests when the series of room-corner tests were done.

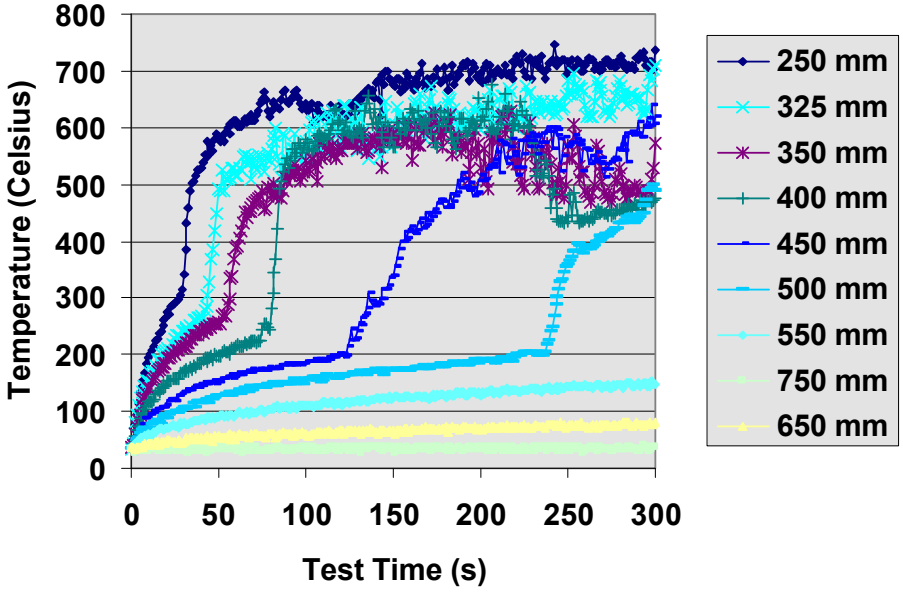

Figure 4—Surface temperatures measured on OSB surface in the LIFT flame travel test.

For the exposure to the 50 kW/m^2 radiant imposed flux at the 50 mm position from the specimen end, the data (not shown) shows surface temperatures profiles at various locations up to 200 mm which is consistent with the flame spread rapidly proceeding downwards from the pilot ignition. In figure 4, the surface temperatures profiles at positions greater than 200 mm is shown in which there was a lateral flame spread that decreased in the travel rate until the flame stopped spreading at around 550 mm. Although it is apparent when the flame has traveled over a thermocouple, it was not apparent as to what the ignition temperature is or just how the temperature rapid rise has occurred just prior to the flame front arrival. Indeed, with the rapid rise in temperature after a radiant preheat period indicates that a small flame-foot heating feature must be captured by a credible model of fire growth.

The typical temperature profiles were easily simulated with the recursive formulation of equation 1 using reasonable heat flux profiles shown in figures 5 and 6 with the corresponding temperatures predictions in figures 7 and 8 in comparison with the data. The thermophysical properties for OSB were taken from our previous ignitability results. The imposed heat fluxes had three phases to properly predict surface temperatures. The first phase is the few seconds increase in heat flux as a result of sliding the specimen into place. At the 50 mm location where the radiant flux was set at about 50 kW m^2, the calculated temperature response reached 301 °C at 12 seconds in figure 7. The third phase of heat flux is caused by the flame foot modeled with time-changing form of equation 5, having the flame foot heat flux of 60 kW/m^2 and a time constant of 0.4 seconds. The rapid exponentially upturn of the temperature was captured using 0.2 seconds time steps so that the surface temperature of 408 °C was obtained at 15.4 seconds (flame sheet arrival time). Further, but damped, temperature rise was in response to the imposed flux set at 110 kW/m^2. Similar pattern is noted for figure 8, which required a flame foot heat flux of 60 kW/m^2, time constant of 4.0 seconds, and flame sheet arrival time at 83 seconds. With the relative increase of the time constant by 10 times, meant that the local flame travel rate at 50 mm is also 10 times of that at 200 mm. Note that the net surface heat flux due to surface emitting radiation and reduction in convection heat flux has rapidly changing profile adequately captured by the analytical model to predict the temperature response.

It is interesting that no charring of the wood surface was needed for making close temperature predictions, allowing us to take the planned steps to validate the lateral flame travel rate formula given by equation 7. Since we have measurements from the thermopile in the flue gas and from fume stack thermocouple (ASTM E1317), we can derive the sensible HRR profile (Dietenberger 1994) and compare it with the model estimated HRR profile from equation 14. Success with this approach can be applied to other situations involving flame travel opposing the air flow, such as ground flame propagation or fire on a deck surface.

Selected Room-Corner Tests

Because the analytical fire growth model for changing conditions differs somewhat from the original model, we decided to focus on predicting the upward fire growth behavior in corner walls, particularly if no fudging of material properties was required and that it provided a good representation of the exterior environment (far below the flashover conditions). In the case

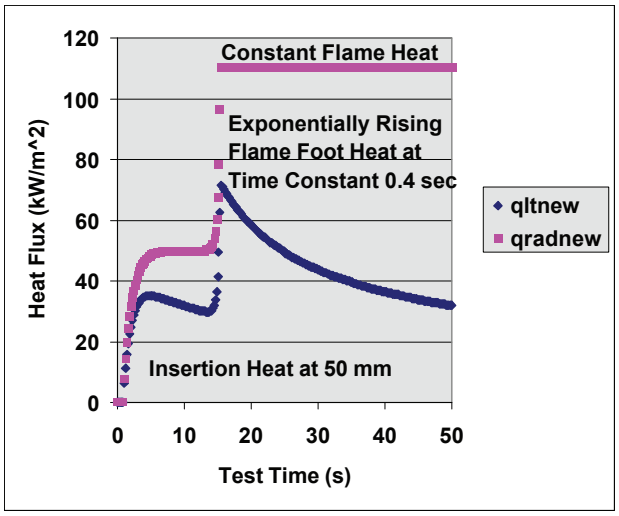

Figure 5—Imposed heat fluxes modeled for temperature predictions at the 50 mm location.

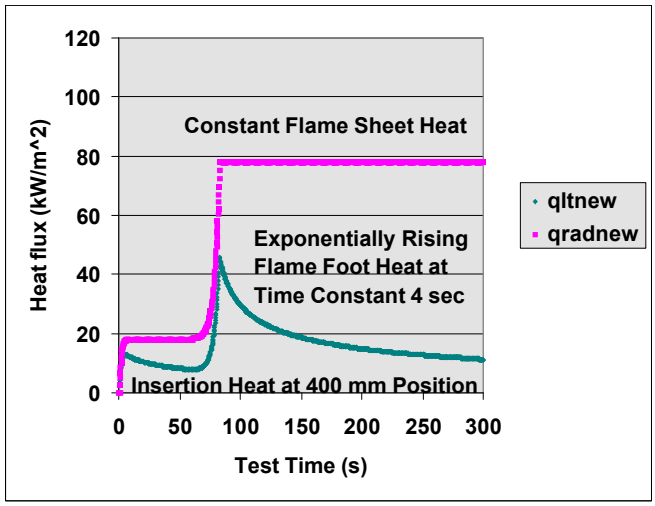

Figure 6—Imposed heat fluxes modeled for temperature predictions at the 400 mm location.

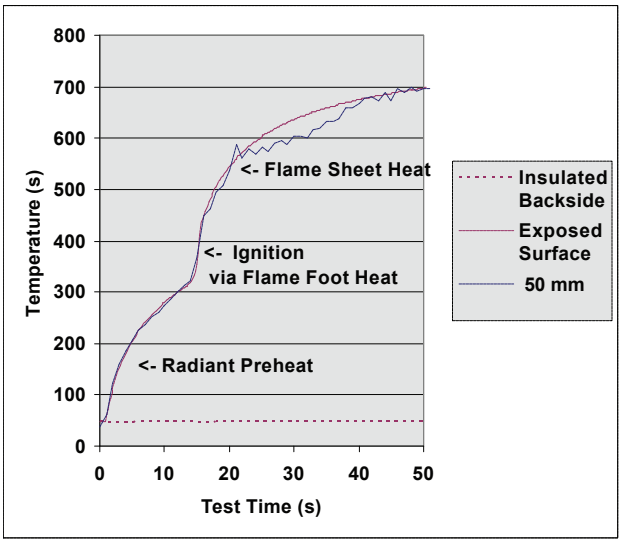

Figure 7—Prediction of measured surface temperature using imposed heat fluxes in figure 5.

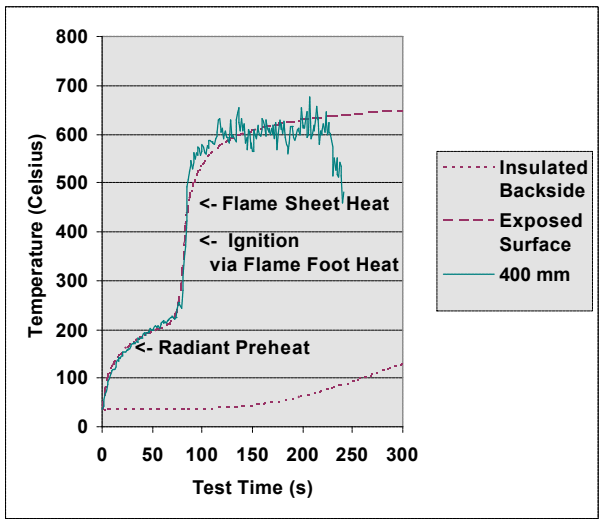

Figure 8—Prediction of measured surface temperature using imposed heat fluxes in figure 6.

of OSB we used the properties published earlier (Dietenberger and Grexa 1996). Figure 9 shows our Room-Corner flashover test with OSB linings on the walls and gypsum board on the ceiling. We also show with the dotted smooth curve the ignition burner going to 100 kW as it is observed by the gas analyzers, in which we take into account gas mixings in the test room and gas sensors and time travel of the sampled gas to the sensors. The OSB ignited 25 seconds after exposure to the ignition burner and led to an upward fire growth that is shown as the HRR profile rising above that of the ignition burner. The dashed smooth curve is predicted by equation 14 that was also numerically filtered with a time constant of 18 sec for gas lag in the

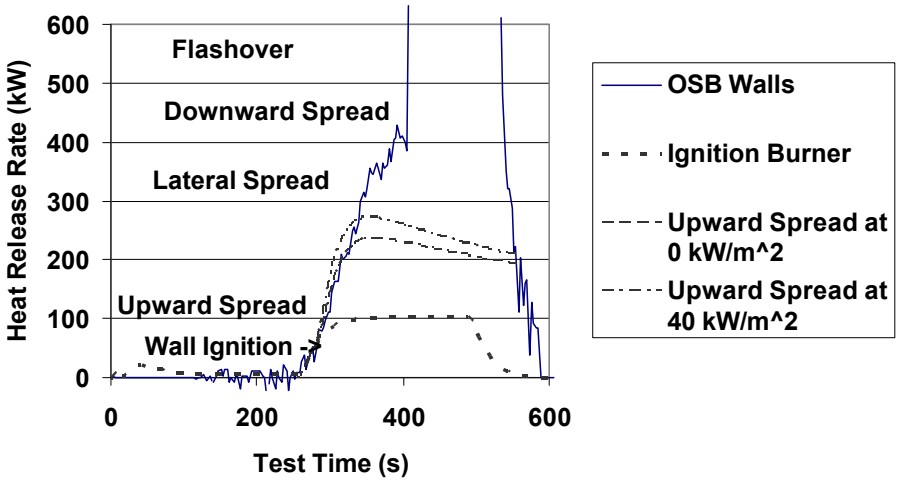

Figure 9—Analytical prediction and Room-Corner test for OSB on the walls that varies the external radiant flux from 0 to 40 kW/m^2.

room and a time constant of 10 seconds for the gas lag in the sensors. The dot-dashed smooth curve is the result of applying an external radiant flux, 40 kW/m^2, in addition to that from the ignition burner. This ignited the targeted region at about the same time (23.8 seconds) as the ignition burner. The "instantaneous" rise in the HRR to a higher peak HRR (and which has a delayed peak because of the numerical filters required to simulate gas mixings) demonstrate the capability of the recursive analytical fire growth model to adapt to changing conditions. Several other examples of changing conditions have been applied that showed reasonable results (not shown). Another type of changing conditions we have recently simulated is the effect of fire resistive linings on reducing and even stopping upward fire growth. Our examples include FRT polyurethane foam, FRT plywoods and the Type X gypsum board (shown at the conference presentation).

Conclusions

The introductory discussions on wildfire threats to construction and their mitigation have shown the need to understand damage, ignition, and fire growth as exposed to changing conditions on realistic combustible items, including those considered to be fire resistive. The calculations should ultimately be able to provide (1) the fuel clearance (both vegetation and structure) needed for mitigating large fire threats of high radiant flux/flame impingements on structures and (2) the mitigation of firebrand threat (from both woodland and neighborhood) to an uninvolved structure with several different and economical fire resistive claddings. Thus far we show how the use of data from the bench scale Cone Calorimeter and of various flame travel tests such as LIFT, Room-Corner test, Radiant Panel, and so on can be used in analytically based fire growth models adaptable to changing conditions. We believe that by providing a fire hazard tool based on fire growth algorithms associated with ornamental vegetations and fire resistive exteriors in changing environments as proposed here, that the client will be able to find an optimum and economical fire-safe construction and landscaping.

References

Dietenberger, Mark A. 1991. Piloted Ignition and Flame Spread on Composite Solid Fuels in Extreme Environments. Ph.D. Dissertation. Dayton, OH: University of Dayton.

Dietenberger, Mark A. 1994. Protocol for Ignitability, Lateral Flame Spread, and Heat Release Rate Using Lift Apparatus. In: Nelson, Gordon L. ed. Fire and polymers II. Materials and tests for hazard prevention: Proceedings of 208th National meeting of the American Chemical Society. August 1994. http://www.fpl.fs.fed.us/documnts/pdf1995/diete95c.pdf

Dietenberger, Mark A. 2006a. Analytical Modeling of Fire Growth on Fire-Resistive Wood-based Materials with Changing Conditions. In: 17th Annual BCC Conference on Flame Retardancy, May, 2006, Stamford, CT. Norwalk, CT: Business Communications Co.

Dietenberger, M.A. 2006b. Using a Quasi-Heat-Pulse Method to Determine Heat and Moisture Transfer Properties for Porous Orthotropic Wood Products. Journal of Thermal Analysis and Calorimetry Vol. 83, No. 1: 97-106.

Dietenberger, M.A.; Grexa, O. 1996. Analytical Model of Flame Spread in Full-Scale Room/Corner Tests (ISO9705), 6th Int. Fire & Materials Conf., San Antonio, TX, Feb. 22-23, Interscience Comm. Ltd.: 211-222.

Karlsson, Bjorn. 1993. A Mathematical Model for Calculating Heat Release Rate in the Room Corner Test. Fire Safety Journal.Vol. 20: 93-113.

Manzello, S.L.; Cleary, T.G.; Shields, J.R.; Yang, J.C. 2006. On the Ignition of Fuel Beds by Firebrands. Fire and Materials Vol. 30: 77-87.